

May 15, 1993

## Nonreciprocal coupling structure of dielectric wave-guides

P. Kwan

C. Vittoria  
*Northeastern University*

J. Proske

---

### Recommended Citation

Kwan, P.; Vittoria, C.; and Proske, J., "Nonreciprocal coupling structure of dielectric wave-guides" (1993). *Electrical and Computer Engineering Faculty Publications*. Paper 96. <http://hdl.handle.net/2047/d20002267>



## Nonreciprocal coupling structure of dielectric wave guides

P. Kwan, C. Vittoria, and J. Proske

Citation: *J. Appl. Phys.* **73**, 7012 (1993); doi: 10.1063/1.352414

View online: <http://dx.doi.org/10.1063/1.352414>

View Table of Contents: <http://jap.aip.org/resource/1/JAPIAU/v73/i10>

Published by the [American Institute of Physics](#).

---

### Related Articles

Reducing vortex losses in superconducting microwave resonators with microsphere patterned antidot arrays  
*Appl. Phys. Lett.* **100**, 012601 (2012)

On chip complex signal processing devices using coupled phononic crystal slab resonators and waveguides  
*AIP Advances* **1**, 041903 (2011)

A novel scaling law relating the geometrical dimensions of a photocathode radio frequency gun to its radio frequency properties  
*Rev. Sci. Instrum.* **82**, 123304 (2011)

Whispering gallery modes for elastic waves in disk resonators  
*AIP Advances* **1**, 041902 (2011)

Negative capacitor paves the way to ultra-broadband metamaterials  
*Appl. Phys. Lett.* **99**, 254103 (2011)

---

### Additional information on *J. Appl. Phys.*

Journal Homepage: <http://jap.aip.org/>

Journal Information: [http://jap.aip.org/about/about\\_the\\_journal](http://jap.aip.org/about/about_the_journal)

Top downloads: [http://jap.aip.org/features/most\\_downloaded](http://jap.aip.org/features/most_downloaded)

Information for Authors: <http://jap.aip.org/authors>

## ADVERTISEMENT

**LakeShore Model 8404** developed with **TOYO Corporation**  
**NEW AC/DC Hall Effect System** Measure mobilities down to 0.001 cm<sup>2</sup>/V s

# Nonreciprocal coupling structure of dielectric wave guides

P. Kwan and C. Vittoria

Department of Electrical and Computer Engineering, Northeastern University, Boston, Massachusetts 02115

J. Proske

Stackpole Inc., Magnet Division, Kane, Pennsylvania 16735

*M*-type hexagonal ferrites have been incorporated in a coupled dielectric image guides structure for nonreciprocal microwave circuits design. Two different field configurations have been considered in this paper: for case I the *c* axis of the ferrite materials was aligned along the direction of propagation; for case II the *c* axis was aligned in the transverse direction. Electromagnetic wave scattering *S* parameters of the device were measured for an external biasing magnetic field applied parallel and perpendicular to the *c* axis of the ferrite slab. We have observed nonreciprocal microwave effects in the ferromagnetic resonance regime as a result of a nonuniform external biasing magnetic field along the propagation direction. We believe that ferrite devices operating at millimeter-wavelength frequencies, such as isolators, filters, modulators, switches, phase shifter, etc., can be implemented from our device design.

In this article we report on the measurement of the scattering parameters for the device configuration shown in Fig. 1 in which the ferrite of choice is a hexagonal ferrite for the purpose of reducing the external field requirements for operation between 26 and 40 GHz. The polycrystal ferrite slab was specially prepared (sintered) so that the remanence magnetization was along the *c* axis. However, approximately 85% orientation of the *c* axis was achieved during sintering of the ferrite. The ferrites had a substantial remanence magnetization along the *c* axis that could provide ferromagnetic resonance (FMR) at the microwave frequency regime with zero external biasing field. The *c* axis of the ferrite is also defined as the easy axis of magnetization in the ferrite slab ( $\text{BaFe}_{12-2x}\text{Co}_x\text{Ti}_x\text{O}_{19}$ ). In case I, the external biasing field **H** was parallel to the direction of propagation, and in case II, **H** was transverse to the direction of propagation, but normal to the ground plane.

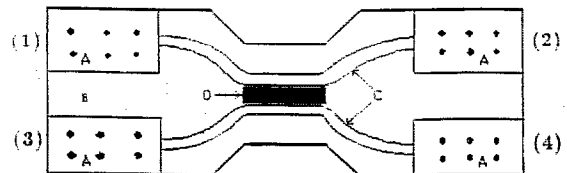
The device configuration of Fig. 1 was chosen due to its simplicity of fabrication and analysis. The frequency range of interest was 26.5–40.0 GHz. Insertion loss of a passive device is one of the major factors that one must consider in millimeter-wave circuit designs. For dielectric image lines, there are four types of losses that we need to consider: dielectric, magnetic, conduction, and radiation. Dielectric losses scale nearly linearly with frequency as pointed out by Xia *et al.*<sup>1</sup> In order to minimize dielectric loss, a dielectric material with low loss tangent was chosen for the device. Hence, Teflon was used [ $\epsilon = 2.25(1 - j1 \times 10^{-4})$ ] with rectangular cross-section dimensions of  $1.9 \times 1.7$  mm.<sup>1</sup> For these dimensions the corresponding cutoff frequency was approximately 22.5 GHz for the fundamental mode of propagation.

In general, nonreciprocal microwave devices make use of ferrimagnetic materials to couple the electromagnetic energy to the precessional motion of the ferrite. In our device, *M*-type hexagonal ferrite ( $\text{BaFe}_{12-2x}\text{Co}_x\text{Ti}_x\text{O}_{19}$ ) with a self-biasing field was chosen. Magnetic loss was relatively small in comparison to radiation. Typically, radiation losses were 7 dB and the magnetic losses were approximately 1 dB. The main advantage of this type of ferrite is

that it provided ferromagnetic resonance without any external biasing field. However, in order to observe nonreciprocal effects, only a small nonuniform magnetic field was required in our design. The physical parameters of the ferrite slab are given in Table I.

In our experimental work, a HP8510B Vector Network Analyzer was used for measuring the scattering parameters. Experimental measurements were performed in the frequency range 26.5–40.0 GHz. When the external biasing field was fixed in a given direction, we observed effects due to FMR in the scattering *S* parameters. This technique was very helpful in terms of analyzing the nonreciprocal behavior of our device. Nonreciprocal behavior was defined as follows:<sup>2</sup> If  $S_{ij}$  is different from  $S_{ji}$  with the direction of the external magnetic field fixed, then the device behaves nonreciprocally.

In case I, the *c* axis of the ferrite slab was placed in the direction of propagation with the external magnetic field applied parallel to it. We reported here the electromagnetic scattering *S* parameters for the magnetic field distributions of  $H_{\text{max}} = 325$  Oe and  $H_{\text{min}} = 175$  Oe in the direction of propagation.



- A. - Waveguide Port (Launcher)
- B. - Ground Plane
- C. - Dielectric Image Guide
- D. - Ferrite

FIG. 1. The top view of the device structure without the top conducting plate.

TABLE I. The characteristics of the ferrite slab and the amount of attenuation for cases I and II.

Characteristics	Case I	Case II
Length	2.05 cm	2.79 cm
Width	0.30 cm	0.30 cm
Thickness	0.165 cm	0.163 cm
$4\pi M_s$ (Oe)	3000.0	3000.0
$H_A$ (Oe)	11600.0	11600.0
$\epsilon_r$	13.0	13.0
$H_{max}$ (Oe)	325	550
$H_{min}$ (Oe)	175	425
$(S_{21})$ (dB)	28.0	50.0
$(S_{12})$ (dB)	42.0	29.0
$(S_{41})$ (dB)	38.0	50.0
$(S_{14})$ (dB)	—	42.5

For this field direction the coupling between the ferrite material and microwave field is maximum, since the magnetization is perpendicular to the strongest component of the rf magnetic field. The rf field direction is transverse to the propagation direction. As such, nonreciprocal effects are enhanced. The form of the scattering matrix for this case takes the following form:

$$[S] = \begin{pmatrix} S_{11} & S_{12} & S_{13} & S_{14} \\ S_{21} & S_{11} & S_{41} & S_{24} \\ S_{31} & S_{14} & S_{11} & S_{12} \\ S_{41} & S_{42} & S_{21} & S_{11} \end{pmatrix} \quad (1)$$

The diagonal elements of  $[S]$  are the reflection coefficients, and the off-diagonal elements corresponding to the transmission parameters. From the theoretical point of view,  $S_{22}$  is not equal to  $S_{11}$  for a nonreciprocal device. In our experimental setup, the measured signal strength for  $S_{11}$  and  $S_{22}$  were very weak; therefore, it was hard to distinguish the difference between  $S_{11}$  and  $S_{22}$ . Similar results were obtained for  $S_{33}$  and  $S_{44}$ .

In order to characterize the four-port device fully, 12 independent measurements are needed. However, our primary interest is the nonreciprocal behavior. We measured two resonances in  $S_{12}$  [Fig. 2(a)]. We attribute the resonance behavior to magnetostatic wave excitation in the ferrite slab.<sup>3</sup> For the forward transmission  $S_{21}$ , the resonances are not as pronounced as  $S_{12}$ . Below FMR, differential phase change was about  $80^\circ$  for  $S_{21}$  [see Fig. 2(b)], and the corresponding attenuation was approximately 12 dB. However, the phase shift was greater than  $100^\circ$  above resonance for  $S_{12}$  and the loss was about 10 dB [Fig. 2(b)]. We believe that the amount of attenuation can be reduced if radiation loss can be reduced.

In addition there was strong coupling between ports 1 and 4 [see Fig. 2(c)]. The amount of coupling was a function of the separation between the two image lines, operating frequencies, etc. The insertion loss for  $S_{14}$  was minimal at all frequencies, including frequencies near FMR [see Fig. 2(b)]. However, FMR had a very strong effect on the forward coupling ( $S_{41}$ ). The difference in propagation loss between  $S_{14}$  and  $S_{41}$  at FMR frequency was approximately

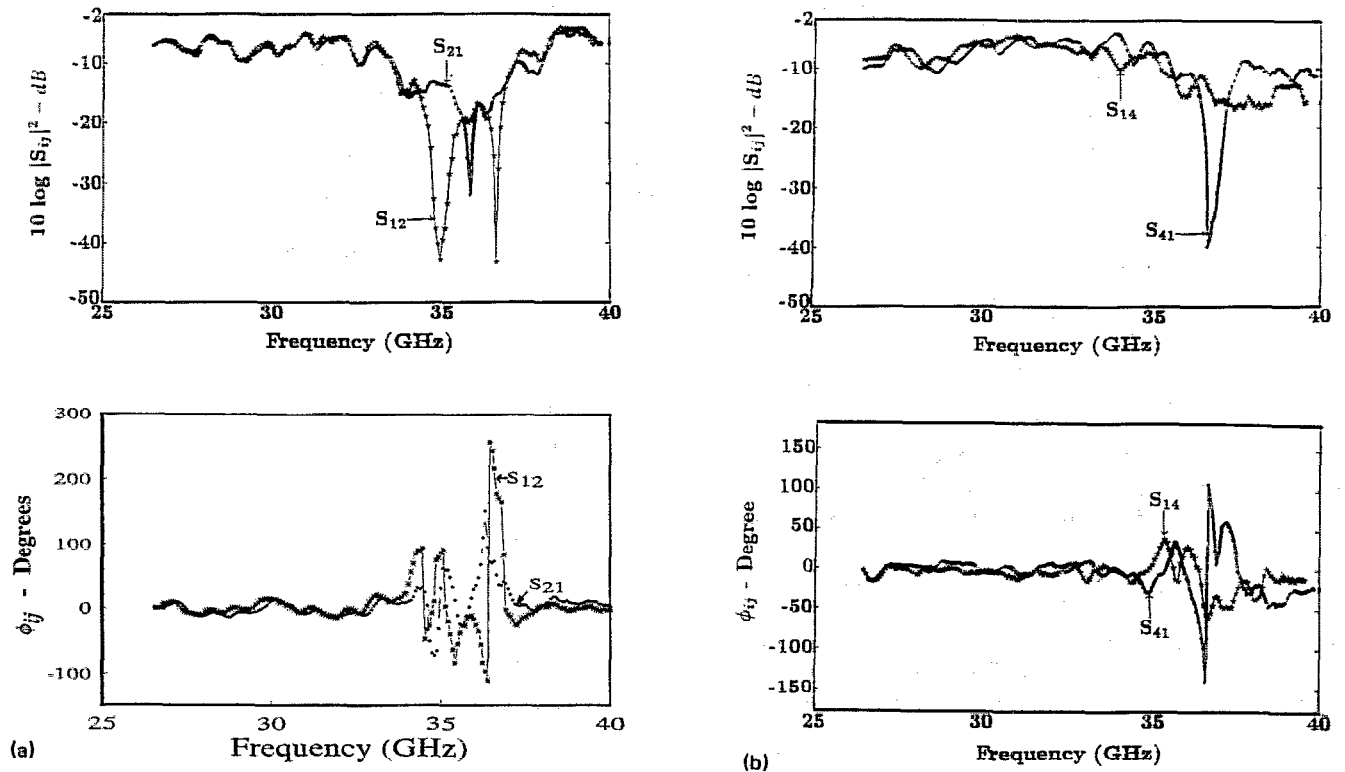


FIG. 2. (a) The magnitude of forward and reverse transmission for case I. (b) Differential phase change in forward and reverse transmission for case I. (c) The magnitude of forward and reverse coupling for case I. (d) Differential phase change in forward and reverse coupling for Case I.

30 dB. Also, above FMR frequency we observed more than 50° of phase shift between the coupling ports [see Fig. 2(d)]. For phase-shifting applications, operation is suggested at frequencies below or above that for FMR. Thus, it is possible to achieve a maximum phase shift with minimum insertion loss.

Finally, for this field configuration, we observed very strong nonreciprocal behavior due to FMR in the forward transmission and coupling ports. The FMR frequency for  $S_{41}$  was different from  $S_{21}$ ; the shift in FMR frequency was due to phase matching between the ferrite slab and the dielectric image guide as electromagnetic energy coupled through the ferrite material. Phase matching was due to the fact that the dielectric constant for Teflon was 2.25 and the dielectric constant for the ferrite slab was 13. There appears to be evidence for circulation behavior in the device, as indicated in Fig. 2.

For this case, the  $c$  axis of the ferrite slab was oriented transverse to the direction of propagation, and parallel to the ground plane. When the external magnetic field was applied perpendicular to the ground plane, the scattering  $S$  parameters were measured. The  $E^y$  mode of propagation occurs in the guided structure. For this mode of excitation, the magnetic fields are linearly polarized irrespective of propagation direction. Hence, reciprocal behavior was observed in the absence of external biasing field, since  $M_s$  and  $h_{rf}$  are parallel to each other. However, we may alter the special coupling symmetry by applying an external applied magnetic field normal to  $h_{rf}$ . In this field configuration, we anticipate less symmetry in the scattering matrix due to the fact that the  $c$  axis or the dc magnetization is at an oblique angle to  $h_{rf}$ . The form of the scattering matrix for this case takes on the following form:

$$[S] = \begin{pmatrix} S_{11} & S_{12} & S_{13} & S_{14} \\ S_{21} & S_{11} & S_{23} & S_{24} \\ S_{31} & S_{32} & S_{11} & S_{34} \\ S_{41} & S_{42} & S_{43} & S_{11} \end{pmatrix} \quad (2)$$

Again, we observed resonances for  $S_{12}$  and  $S_{21}$  [see Fig. 3(a)]. The other minor resonances occurring at higher frequencies are attributed to magnetostatic wave excitation within the ferrite slab. They are analogies to dimensional resonance in a finite structure. Power absorption in the forward transmission ( $S_{21}$ ) at FMR was more than 50 dB. For coupling ports ( $S_{41}$  and  $S_{14}$ ), very pronounced nonreciprocal effects were observed [see Fig. 3(b)]. From a practical point of view, signals operating in the vicinity of FMR can be switched on and off as in signal processing purposes.

In summary, strong nonreciprocal effects were observed in cases I and II. To our surprise we observed even stronger nonreciprocal effects for case II than for case I. The amount of attenuation at FMR for the transmission ports (1 and 2) and the coupling ports (1 and 4) is summarized in Table I.

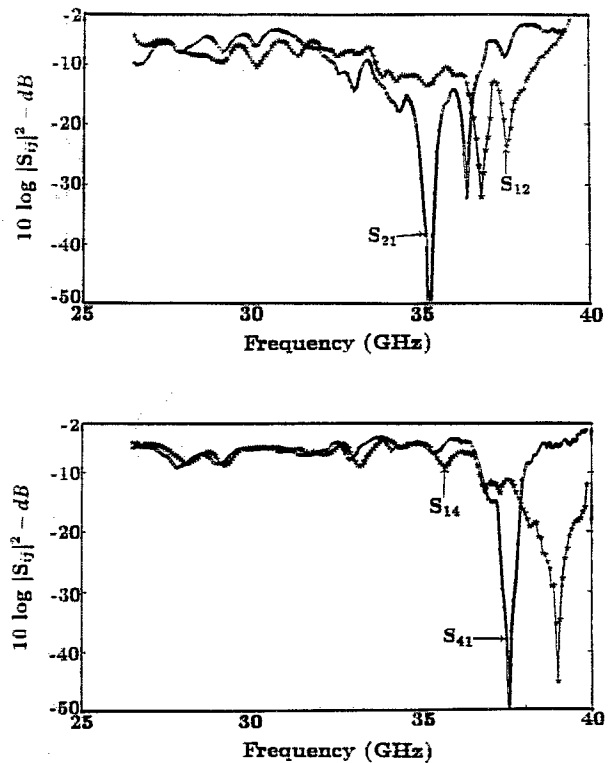


FIG. 3. (a) The magnitude of forward and reverse transmission for case I. (b) The magnitude of forward and reverse coupling for case II.

The forward attenuation ( $S_{21}$ ) was as high as 50 dB at FMR frequency ( $f_0$ ), but the insertion loss ( $S_{12}$ ) was insignificant in comparison to the forward attenuation or vice versa. Thus, the coupling energy is confined to the guided structure. We also observed very strong nonreciprocal effects in the forward coupling ports (ports 1 and 4) at the same time; the return loss was not affected by FMR. This was also true for the forward coupling ports. Phase shifting is one of the applications that can be achieved with our device. For the field configuration normal to the ground plane (case II), the  $E^y$  mode of propagation was conserved or maintained throughout the frequency range investigated. Our device has not been optimized for commercial use. The objective of this research was to demonstrate and explore the feasibility of the device for potential microwave applications. The results presented here could provide a method for nonreciprocal millimeter-wave application deploying planar geometries, such as novel circulators and frequency and phase-tuning devices.

<sup>1</sup> J. Xia, P. P. Toullos, and C. Vittoria, IEEE Trans. Microw. Theory Tech. MTT-37, 1547 (1989).

<sup>2</sup> P. McIsaac, IEEE Trans. Microw. Theory Tech. MTT-24, 223 (1976).

<sup>3</sup> R. W. Damon and J. R. Eshbach, J. Phys. Chem. Solids 19, 308 (1961).